J. Membrane Biol. 193, 91–98 (2003)
DOI: 10.1007/s00232-002-2010-8

The Journal of
Membrane
Biology

Ca^{2+}-activated Nonselective Cation Channels in Rat Neonatal Atrial Myocytes

A.B. Zhainazarov*
Department of Cardiology, Children's Hospital, 320 Longwood Avenue, Boston, MA 02115 and Department of Neurobiology, Harvard Medical School, Boston, MA 02115, USA

Received: 13 December 2002/Revised: 14 February 2003

Abstract. A nonselective cation channel activated by intracellular Ca^{2+} was identified in inside-out membrane patches taken from cultured rat atrial myocytes. Ca^{2+} (0.01–1.00 mM) reversibly activated the channel in a concentration-dependent manner. The channel often showed a quick and irreversible rundown within a few minutes after patch excision. The *I-V* relationship of the channel was linear between −100 and +100 mV. The single channel conductance was 26.0 ± 0.5 pS and its open probability was weakly voltage-dependent. Ion-substitution experiments showed that the channel was permeable to monovalent cations (P_x/P_{Cs}: Li^+ (1.5) = K^+ (1.5) > Na^+ (1.2) > Rb^+ (1.1) > Cs^+ (1.0)) but not to Cl^- (P_{Cl}/P_{Cs} < 0.01) and Ca^{2+} (P_{Ca}/P_{Cs} =0.02 ± 0.01).

Key words: Rat — Electrophysiology — Patch clamp — Single-channel recording — Calcium-activated nonselective cation channels — Cardiac myocyte

Introduction

Single Ca^{2+}-activated nonselective (CAN) cation channels were first described in rat cardiac ventricular myocytes (Colquhoun et al., 1981). CAN channels underlie the transient inward current that is required for rhythmic activity in cardiac cells (Kass et al., 1978; Colquhoun et al., 1981). Subsequently, such ion channels were found in a variety of tissues, including neuronal and nonexcitable cells (Partridge & Swandulla, 1988; Siemen, 1993; Thorn & Petersen, 1993). Despite their wide distribution, the molecular identities of these channels, as well as their exact physiological functions, are largely unknown.

Recently, some CAN channels have been suggested to belong to the transient receptor potential (TRP) ion channel family (Petersen, 2002). The TRP gene encoding a Ca^{2+}-permeable cation channel was originally identified in photoreceptors of *Drosophila melanogaster* as an essential component of a light-activated Ca^{2+} channel (Hardie & Minke, 1993). Twenty-two mammalian genes homologous to the TRP gene have been identified (Harteneck, Plant & Schultz, 2000; Clapham, Runnels & Strübing, 2001; Vennekens et al., 2002). These mammalian TRP-related proteins are widely expressed in both nonexcitable and neuronal cells (Montell, Birnbaumer & Flockerzi, 2002). When expressed in heterologous systems, they form ion channels varying significantly in their ion selectivity and mode of activation. TRP channels vary widely in their selectivity to cations, from roughly 100-fold preference for Ca^{2+} over monovalent cations for TRPV5 and TRPV6, to monovalent cation selectivity for TRPM4b. Although mammalian TRP channels have been implicated in a diverse range of physiological processes, their exact functional role is largely unknown.

A member of the TRP channel family, TRPM4b, had very similar biophysical properties to a Ca^{2+}-activated non-selective cation channel when it was overexpressed in HEK-293 cells (Launay et al., 2002). But TRP ion channel proteins expressed in cell lines might behave quite differently in vitro than they do in vivo due to their interactions with either other TRP channels or regulatory proteins endogenous to these heterologous expression systems. Thus, it is important to characterize TRP ion channels in cells where they function in vivo.

Correspondence to: A.B. Zhainazarov; email: abz@ufbi.ufl.edu

**Present address:* UF Center for Smell and Taste, McKnight Brain Institute, University of Florida, 100 S Newell Dr., L1-131, P.O. Box 100015, Gainesville, FL 32610-0015, USA

Knowledge of ion selectivity profiles of CAN channels will be crucial in determining their molecular identities as well as their physiological role(s) in various types of cells. In the experiments described here, I identified a Ca^{2+}-activated nonselective cation channel in rat atrial myocytes. Its permeabilities were directly examined at the single-channel level using excised inside-out patches. I also measured its single-channel conductance, Ca^{2+}- and voltage-dependence.

Materials and Methods

Cell Isolation and Culture

Single atrial myocytes were isolated from the heart of neonatal rat pups (P2; Sprague Dawley) using a neonatal cardiomyocyte isolation kit (Cat# 31D4808; Worthington Biochemical, Lakewood, NJ). Cells were plated on 35-mm culture dishes containing 5-mm glass coverslips. Gelatin (0.1%) was used to coat coverslips. Medium was changed 24 hours after plating. Myocytes were used for experimentation within 1–4 days of culture. Coverslips containing the cells were transferred to a control extracellular solution-filled recording chamber.

Electrophysiological Recordings

Inside-out patch recordings were made as described elsewhere (Hamill et al., 1981). Patch pipettes were fabricated from borosilicate glass (BF150-86-10, Sutter Instruments) using a Flaming-Brown micropipette puller (P-97, Sutter Instruments) and fire-polished to a final tip diameter of less than 1 μM. Pipettes, filled with the patch pipette solution (*see* below for composition), had resistances of 6–10 MΩ; they formed seals on myocyte plasma membranes with resistances of 8–12 GΩ. Single-channel currents were recorded with an Axopatch 200A amplifier (Axon Instruments, Foster City, CA) using a 16-bit data acquisition system (Digidata 1320A, Axon Instruments) and pCLAMP 8.1.0 software (Axon Instruments). Unless otherwise stated, the currents were low-pass filtered at 1–2 kHz (−3 dB; 4-pole Bessel filter) and digitized at 10–20 kHz. The recordings were referenced to an Ag-AgCl wire electrode connected to the bath solution (*see* below for composition) through a 3 M KCl/agar bridge. All potentials were corrected for the liquid junction potentials (Neher, 1992). All experiments were carried out at room temperature (20–22°C).

Data Analysis

The current-voltage relation of single-channel currents was determined by applying voltage ramps (−100 to +100 mV; 300 ms); the resulting currents were digitized and analyzed using the segmented averaging procedure (Heinemann, 1995; Zhainazarov et al., 1998). The reversal potential for any given ionic condition was determined as a point on the voltage axis where the open-channel current-voltage curve intercepted the leakage current-voltage curve.

Unless noted otherwise, results are expressed as the sample mean ± SEM of n observations.

Solutions

The control extracellular solution contained (in mM): 135 NaCl, 5 KCl, 1.8 $CaCl_2$, 1 $MgCl_2$, 5 glucose, 10 HEPES, adjusted to pH 7.4 with NaOH and ~275 mmol/kg osmolarity with glucose. The standard internal solution (nominally Ca^{2+}-free; no added Ca^{2+}) used for the inside-out patch experiments contained (in mM): 140 CsCl, 1 $MgCl_2$, 10 HEPES, 5 glucose, adjusted to pH 7.4 with Tris base and ~275 mmol/kg osmolarity with glucose. The desired free calcium concentrations were achieved by adding an appropriate amount of $CaCl_2$ and EGTA. Free calcium concentrations were calculated with the use of Chelator software (Schoenmakers et al., 1992). In some experiments, part of the CsCl in the standard internal solution was substituted with an equivalent concentration of chloride salts of other alkali metal cations (NaCl, KCl, LiCl, and RbCl). In experiments performed to measure Ca^{2+} permeation through the channel, the internal solution used for the inside-out patch recordings consisted of (in mM) 70 $CaCl_2$, 40 glucose, and 10 HEPES, adjusted to pH 7.4 with Tris base and ~275 mmol/kg osmolarity with glucose. In experiments performed to measure Cl^- permeation through the channel, the internal solution contained (in mM): 28 CsCl, 1 $MgCl_2$, 95 glucose, 10 HEPES, adjusted to pH 7.4 with Tris base and ~275 mmol/kg osmolarity with glucose. Unless noted otherwise, patch pipettes were filled with ionic solution containing (in mM): 140 CsCl, 1 $MgCl_2$, 0.1 $CaCl_2$, 10 HEPES, 5 glucose, adjusted to pH 7.4 with Tris base and ~275 mmol/kg osmolarity with glucose.

All chemicals were purchased from Sigma except for RbCl and glucose, which were obtained from Aldrich Chemical and Fisher Scientific, respectively.

Results

Single-channel Currents Activated by Ca^{2+} in Inside-out Patches from Rat Atrial Myocytes

Ca^{2+} reversibly activated a channel in inside-out patches excised from rat cultured atrial myocytes. An example of Ca^{2+}-evoked unitary currents is illustrated in Fig. 1*A*, where 1 mM Ca^{2+} was applied to the intracellular side of inside-out patches. Such single-channel activity occurred in about 7% of 402 patches tested. Although the channel activity was seen at $[Ca^{2+}]_i$ as low as 10 μM, channel activation was greatest at $[Ca^{2+}]_i \geq 1$ mM. The channel often showed a quick and irreversible rundown within a few minutes after patch excision and the first application of Ca^{2+}. It is likely that the irreversible inactivation of the channel was due to washout or deterioration of crucial components during excised patch recordings. Although rundown prevented us from measuring the complete relationship between the open probability (P_o) and $[Ca^{2+}]_i$, the channel activity level was clearly dependent on $[Ca^{2+}]_i$. When $[Ca^{2+}]_i$ was increased from 100 μM to 1.8 mM, the open probability of the channel increased from 0.33 ± 0.11 (n = 3) to 0.66 ± 0.03 (n = 4) at −80 mV. In the presence of Ca^{2+}, the channel opened to a single level of −1.01 ± 0.02 (n = 6) pA at −46 mV and +1.35 ± 0.04 (n = 3) pA at +54 mV. The channel open probability clearly increased when the membrane potential was changed from negative to positive potentials (Fig. 1*B–D*). For example, the open probability increased from 0.33 ± 0.11 (n = 3) at $[Ca^{2+}]_i$ = 100 μM and

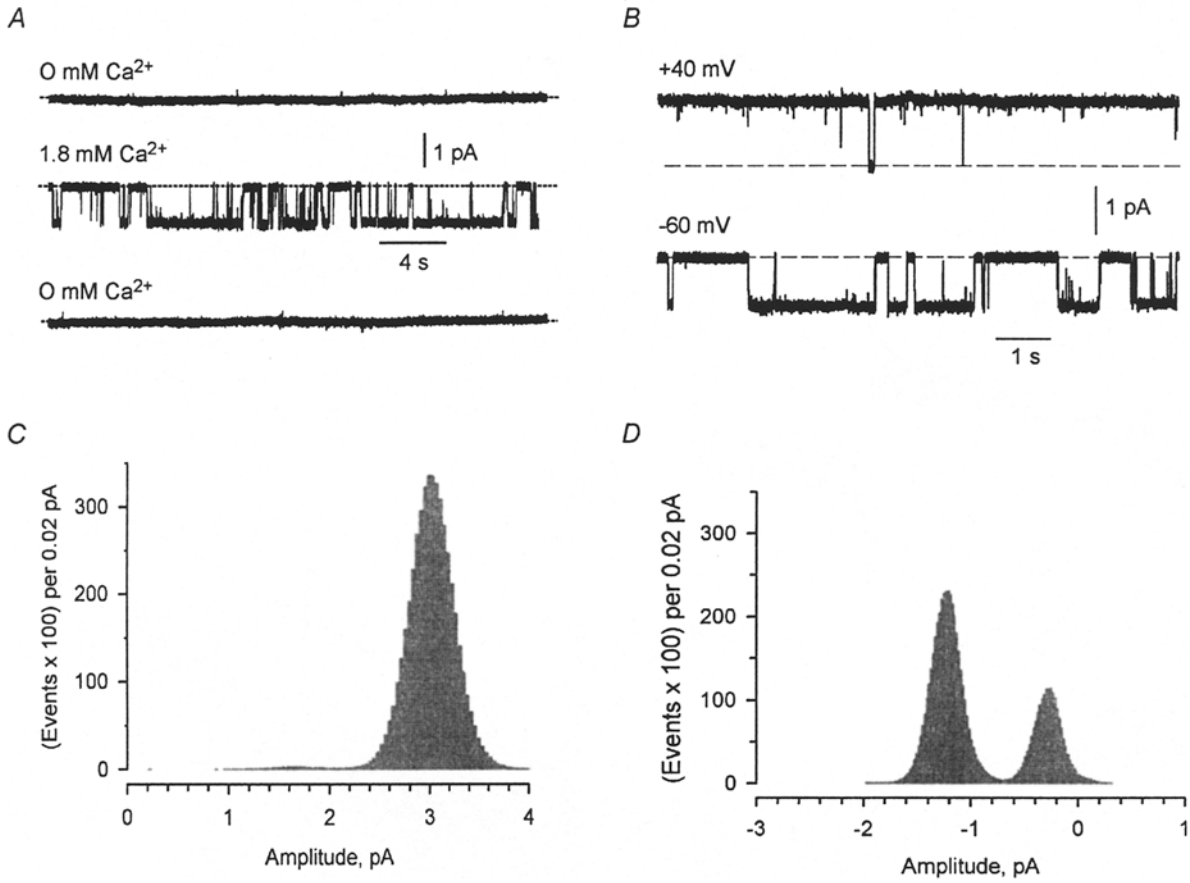

Fig. 1. Ca^{2+} reversibly activates a channel in an inside-out patch from a cultured rat atrial myocyte. (*A*) Representative single-channel records showing the effect of 1 mM Ca^{2+} at a membrane potential of −60 mV. (*B*) Representative segments of the single-channel current traces recorded at two different membrane potentials (upper trace, +40 mV; lower trace, −60 mV). $[Ca^{2+}]_i$ = 1 mM. *C* and *D* are examples of the amplitude histograms of channel openings evoked by 1 mM Ca^{2+} at +40 mV and −60 mV, respectively. The recordings were low-pass filtered at 200 Hz (−3 dB).

0.66 ± 0.03 (n = 4) at $[Ca^{2+}]_i$ = 1.8 mM to 0.56 ± 0.09 (n = 4) at $[Ca^{2+}]_i$ = 100 μM and 0.96 ± 0.03 (n = 4) at $[Ca^{2+}]_i$ = 1.8 mM when the membrane was depolarized from −80 to +60 mV.

Current-voltage Relationship of the Channel

Figure 2*A* illustrates 60 superimposed current traces from the same inside-out patch in response to a voltage ramp from −100 to +100 mV (ramp duration, 300 ms). The patch contained one Ca^{2+}-sensitive channel ($[Ca^{2+}]_i$ = 100 μM). The bath and pipette solutions contained 140 mM CsCl. Figure 2*B* shows an example of both open channel and leakage current-voltage curves obtained from the voltage ramp data (Fig. 2*A*) by using the segmented averaging procedure. The single-channel current reversed its sign at −1.3 ± 0.7 mV (n = 3; Fig. 2*B*). The current-voltage relationship of the channel was linear from −100 to +100 mV (Fig. 2*C*) and its slope conductance was 26.0 ± 0.5 pS (n = 4).

Ion Selectivity of the Channel

Permeability to Cs^+ and Cl^-

Currents through single Ca^{2+}-activated channels in inside-out patches reversed near 0 mV in symmetrical CsCl (140 mM) solution (Figs. 2*B*, 3*A*). To examine the permeability of the channel to Cs^+ and Cl^-, the CsCl concentration bathing the intracellular face of the patch was reduced by 80%. Under these ionic conditions ($[Cs^+]_o$ = 140 mM; $[Cs^+]_i$ = 28 mM; $[Cl^-]_o$ = 142 mM; $[Cl^-]_i$ = 30 mM), the reversal potential of the single channel shifted to positive potentials (ΔE_r = +42 ± 2 mV; n = 3) (Fig. 3*A*, *B*), suggesting that the channel was substantially more permeable to Cs^+ than to Cl^-. The permeability of the Cl^- relative to that of Cs^+ (P_{Cl}/P_{Cs}) was calculated from the shift of the reversal potential (ΔE_r) using the following equation (Hille, 2001)

$$P_{Cl}/P_{Cs} = \{[Cs^+]_i \exp(F\Delta E_r/RT) - [Cs^+]_o\} / \{[Cl^-]_i - [Cl^-]_o \exp(F\Delta E_r/RT)\}, \quad (1)$$

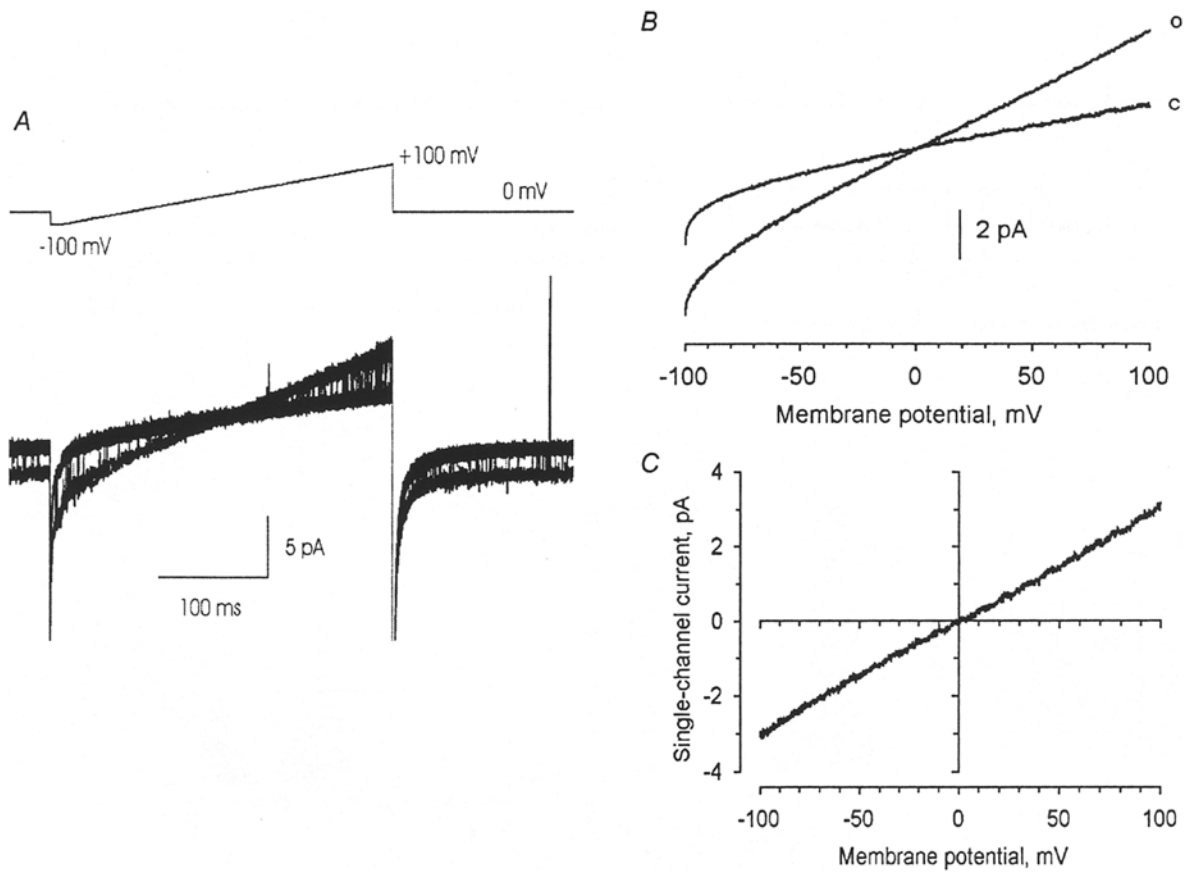

Fig. 2. Current-voltage relation of the Ca^{2+}-sensitive channel. (*A*) Sixty superimposed single-channel current recordings (*lower traces*) evoked by a voltage ramp (*upper trace*). Pipette, 140 mM CsCl. Bath, standard internal solution; $[Ca^{2+}]_i$, 0.1 mM. The recording was low-pass filtered at 1 kHz (−3 dB). (*B*) Relationships between membrane potential and "open channel" (*o*) (leakage (*c*)) current amplitude. The value of reversal potential (0.1 mV) for the channel current is a membrane potential where the "open channel" current-voltage curve intercepts the leak current-voltage curve. Because of the capacitive transients the *I-V* relationships are curved at the left edge of the voltage ramp. (*C*) Current-voltage relationship of the channel obtained by subtracting the leak current-voltage curve from the open-channel current-voltage curve in *B*. Slope conductance was 29.9 pS between −100 and +100 mV.

where F, R, and T have their usual meaning. P_{Cl}/P_{Cs} was less than 0.01, indicating that the channel was highly cation-selective.

Permeability to Ca^{2+}

Permeation of Ca^{2+} through the channel was measured when the intracellular face of the inside-out patch was perfused with a solution containing 70 mM $CaCl_2$ (patch pipette contained 140 mM CsCl). Under these conditions, the single-channel current reversed at very positive membrane potentials (Fig. 4*A*, *B*). Estimates of the reversal potential of the open channel current (E_r) and the permeability of the Ca^{2+} relative to Cs^+ (P_{Ca}/P_{Cs}) were obtained by fitting the open channel current-voltage curve with the following equation (Fatt & Ginsborg, 1958) (Fig. 4*C*)

$$I = I_{Ca} + I_{Cs}. \tag{2}$$

I_{Ca} is a current component due to the movement of Ca^{2+} and given by

$$I_{Ca} = (4P_{Ca}EF^2/RT)[Ca^{2+}]_i/\{1 - \exp(-2EF/RT)\}, \tag{3}$$

where E is the membrane potential. I_{Cs} is a current component due to the movement of Cs^+ and given by

$$I_{Cs} = (P_{Cs}EF^2/RT)[Cs^+]_o \exp(-EF/RT) /\{1 - \exp(-EF/RT)\}. \tag{4}$$

The single-channel current reversed at +74 ± 3 mV (n = 3) and the permeability ratio of the Ca^{2+} relative to Cs^+ (P_{Ca}/P_{Cs}) was 0.02 ± 0.01 (n = 3), indicating that the channel is not substantially permeant to Ca^{2+}.

Permeability to Alkali Metal Cations

To determine the ionic selectivity of the channel, we perfused the intracellular face of the inside-out patch with 140 mM of one of the following monovalent

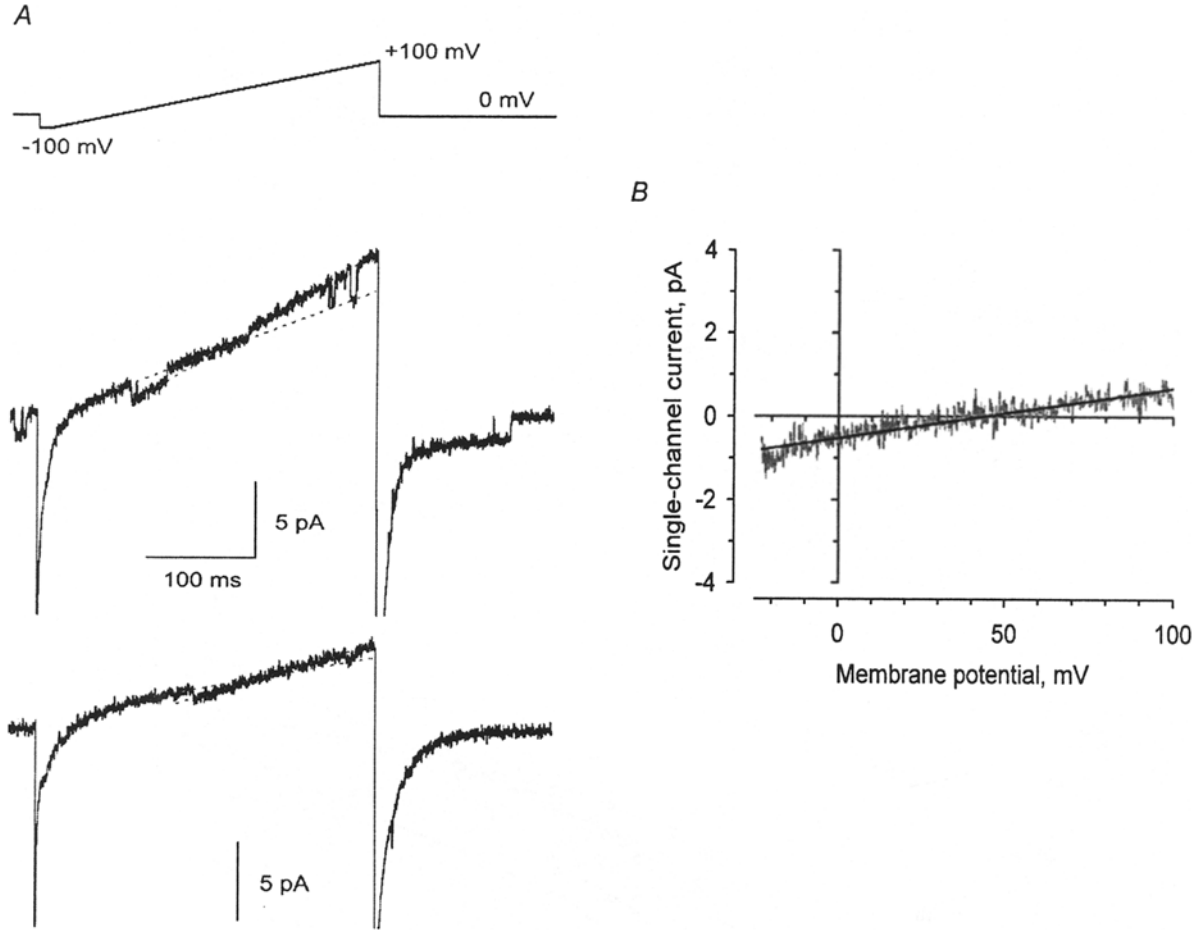

Fig. 3. Permeability of Cl^- through the channel. (*A*) Single-channel current recordings evoked by a voltage ramp (*top trace*) in the presence of either 142 mM (*middle trace*) or 32 mM (*bottom trace*) $[Cl^-]_i$. $[Ca^{2+}]_i$, 1 mM. The recording was low-pass filtered at 1 kHz (−3 dB). (*B*) Relationship (*gray trace*) between membrane potential and single-channel current amplitude when $[Cl^-]_i$ was 32 mM. Pipette, 140 mM Cl^-. *Black solid line*, linear regression through data points.

cations: K^+, Na^+, Li^+, Rb^+, and Cs^+. The patch pipette contained 140 mM Cs^+. Under these ionic conditions, the reversal potential (E_r) of the open-channel current measured by applying voltage ramps (−100 to +100 mV; 300 ms) was −10.5 ± 0.5 mV (n = 6) for K^+, −5.0 ± 0.1 mV (n = 3) for Na^+, −1.3 ± 0.7 mV (n = 3) for Cs^+, −3.1 ± 1.0 mV (n = 3) for Rb^+, and −10.5 ± 0.6 mV (n = 6) for Li^+ (Fig. 4*D*). The permeability of the test monovalent ion X^+ relative to that of Cs^+ (P_X/P_{Cs}) was calculated from the shift of the reversal potential (ΔE_r) by using the Goldman-Hodgkin-Katz "voltage" equation (Hille, 2001)

$$\Delta E_r = (RT/F)\ln\{(P_{Cs}[Cs^+]_o)/(P_X[X^+]_i)\}, \quad (5)$$

where $[X^+]_i$ is the intracellular concentration of the cation X^+. The permeability ratio sequence (P_X/P_{Cs}) was Li^+ (1.5) = K^+ (1.5) > Na^+ (1.2) > Rb^+ (1.1) > Cs^+ (1.0), indicating that the channel is fairly nonselective among alkali metal cations.

Discussion

In the present study, I have identified and characterized a nonselective cation channel in primary cultures of atrial myocytes obtained from neonatal rat heart. The channel is specifically activated by intracellular Ca^{2+} in excised inside-out patches. Similar Ca^{2+}-activated nonselective cation channels have previously been reported to occur in ventricular myocytes of both neonatal (Colquhoun et al., 1981) and adult rats (Guinamard et al., 2002), and adult guinea pigs (Ehara et al., 1988). The channel from rat atrial myocytes has a single-channel conductance of 26 pS, which is close to the value of conductance reported for ventricular myocytes from adult rats (26.5 pS; Guinamard et al., 2002). The channel conductance was only 14.8 pS for ventricular myocytes from guinea pigs (Ehara et al., 1988) and in the range of 30–50 pS for ventricular myocytes from neonatal rats (Colquhoun et al., 1981). All these channels are relatively nonselective for Na^+ and K^+ and highly

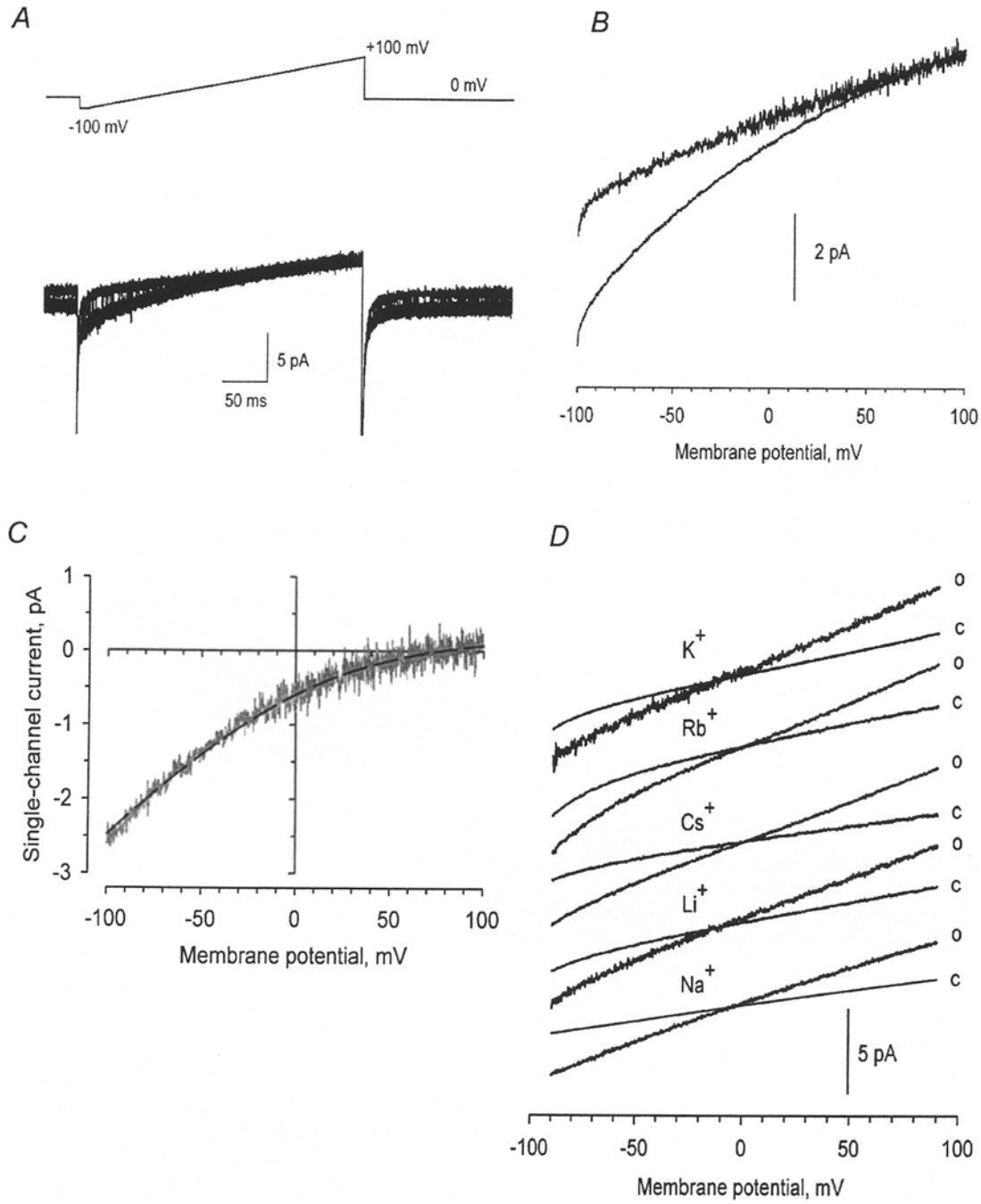

Fig. 4. Permeability of Ca^{2+} and alkali metal cations through the channel. (*A*) 60 superimposed single-channel current recordings (*lower traces*) evoked by a voltage ramp (*upper trace*). Pipette; 140 mM CsCl; bath, 70 mM $CaCl_2$. The recording was low-pass filtered at 1 kHz (−3 dB). (*B*) Relationship between membrane potential and "open channel" (*upper trace*) (leakage (*lower trace*)) current amplitude. (*C*) The current-voltage relationship (*gray trace*) of the channel obtained by subtracting the leak current-voltage curve from the open-channel current-voltage curve in *B*. The dashed line is the fit of Eq. (2) to the data points. (*D*) Permeability of alkali metal cations through the channel. The reversal potential of the channel current was defined as the membrane potential where the "open channel" current-voltage curve (*o*) intercepted the leak current-voltage curve (*c*). Bath solution, 140 mM of one of the following alkali metal chloride: KCl, RbCl, CsCl, LiCl, and NaCl. $[Ca^{2+}]_i$, 0.1 mM. Patch pipette, 140 mM CsCl. The open-channel current reversed its polarity at: −11.2 mV for K^+; −2.1 mV for Rb^+; 0.1 mV for Cs^+; −11.2 mV for Li^+; and −5.1 mV for Na^+, respectively. The recording was low-pass filtered at 1 kHz (−3 dB). Bath: standard internal solution; $[Ca^{2+}]_i$, 1 mM.

impermeable to both Ca^{2+} and Cl^-. In my study, the open probability of the CAN channel increased with membrane depolarization, which is similar to the data observed in ventricular myocytes from adult rats (Guinamard et al., 2002). But the open probabilities of the CAN channels recorded in ventricular myo-

cytes from adult guinea-pig and neonatal rat hearts were voltage-independent in the range from −100 mV to +60 mV (Ehara et al., 1988; Colquhoun et al., 1981).

There was also variability in the Ca^{2+}-dependence of the CAN channel open probability. In ventricular myocytes from adult guinea-pig hearts, the open probability of the CAN channel was increased by raising $[Ca^{2+}]_i$ with a half-maximum concentration of 1.2 μM (Ehara et al., 1988). In my study, although the channel activity was seen at Ca^{2+} concentrations as low as 10 μM, substantial channel activation was only observed at $[Ca^{2+}]_i \geq 1$ mM, which is similar to the Ca^{2+} sensitivity observed for CAN channels in ventricular myocytes from both neonatal and adult rat hearts (Colquhoun et al., 1981; Guinamard et al., 2002).

Most cardiac CAN channels studied so far exhibit a quick and irreversible rundown of their activities within a few minutes after patch excision, indicating that there are intracellular factors required for its activation. Guinamard et al. (2002) reported that the CAN activity in cultured rat ventricular cardiomyocytes was reduced by intracellular ATP. In the present study the intracellular solutions did not contain ATP. It is possible that the cardiac CAN channels are modulated by the metabolic state of the cell, as was proposed for a number of other cell types (Koivisto et al., 1998; Kamouchi et al., 1999; Suh et al., 2002). Notwithstanding the above-stated differences in the reported single-channel properties, it is clear that cardiac myocytes from two different species at two different developmental stages express a nonselective cation channel activated by intracellular Ca^{2+}.

Although the physiological significance of CAN channels is unknown, they are candidates for the transient inward current that develops in Ca^{2+}-overloaded cardiac cells (Kass et al., 1978). Recently, it has been suggested that the CAN channels might be involved in sustained depolarization associated with cardiac hypertrophy and eventually arrhythmias (Guinamard et al., 2002).

Recently, it has been reported that TRPM4b, a member of the TRP family, forms a homomultimeric, Ca^{2+}-activated nonselective cation (CAN) channel when overexpressed in HEK-293 cells (Guinamard et al., 2002). As judged from Northern blot analysis, TRPM4b gene is widely expressed in a variety of tissues, including heart. The TRPM4b channel has a conductance of 25 pS and is directly activated by $[Ca^{2+}]_i \geq 0.3$ μM. The TRPM4b is impermeable to Ca^{2+} and does not discriminate well between Na^+ and K^+. Guinamard and coworkers propose that TRPM4a is a CAN channel activated following receptor-mediated Ca^{2+} mobilization, but they also report that TRPM4b is expressed in HEK-293 cells endogenously. In principle, it is possible that TRPM4b does not form a CAN channel, but that its overexpression upregulates a function of another CAN channel native to HEK-293 cells. Although TRPM4b is a likely molecular candidate for a CAN channel, the molecular nature of the CAN channel is still an open question.

This work was done in Dr. D.E. Clapham's laboratory at Children's Hospital and supported by the Howard Hughes Medical Institute. I thank C. Roberson and Q. Shi for their invaluable help with the preparation of the cultured atrial myocytes. I am also thankful to Dr. D.E. Clapham for his encouragement and helpful comments on the manuscript.

References

Clapham, D.E., Runnels, L.W., Strübing, C. 2001. The trp ion channel family. *Nature Rev. Neurosci.* **2:**387–396

Colquhoun, D., Neher, E., Reuter, H., Stevens, C.F. 1981. Inward current channels activated by intracellular Ca in cultured cardiac cells. *Nature* **294:**752–754

Ehara, T., Noma, A., Ono, K. 1988. Calcium-activated non-selective cation channel in ventricular cells isolated from adult guinea-pig hearts. *J. Physiol.* **403:**117–133

Fatt, P., Ginsborg, B.L. 1958. The ionic requirements for the production of action potentials in crustacean muscle fibres. *J. Physiol.* **142:**516–543

Guinamard, R., Rahmati, M., Lenfant, J., Bois, P. 2002. Characterization of a Ca^{2+}-activated nonselective cation channel during dedifferentiation of cultured rat ventricular cardiomyocytes. *J. Membrane Biol.* **188:**127–135

Hamill, O.P., Marty, A., Neher, E., Sakmann, B., Sigworth, F.J. 1981. Improved patch-clamp techniques for high-resolution current recording from cells and cell-free membrane patches. *Pfluegers Arch.* **391:**85–100

Hardie, R.C., Minke, B. 1993. Novel Ca^{2+} channels underlying transduction in *Drosophila* photoreceptors: implications for phosphoinositide-mediated Ca^{2+} mobilization. *TINS* **16:**371–376

Harteneck, C., Plant, T.D., Schultz, G. 2000. From worm to man: three subfamilies of TRP channels. *TINS* **23:**159–166

Heinemann, S.H. 1995. Guide to data acquisition and analysis. *In:* Single-Channel Recording. Second edition. B. Sakmann and E. Neher, editors, pp. 53–471. Plenum, New York

Hille, B. 2001. Ionic Channels of Excitable Membranes. Second edition. Sinauer Associates, Inc., Sunderland, MA

Kamouchi, M., Mamin, A., Droogmans, G., Nilius, B. 1999. Nonselective cation channels in endothelial cells derived from human umbilical vein. *J. Membrane Biol.* **169:**29–38

Kass, R.S., Lederer, W.J., Tsien, R.W., Weingart, R. 1978. Role of calcium ions in transient inward currents and after contractions induced by strophanthidin in cardiac Purkinje fibres. *J. Physiol.* **281:**187–208

Koivisto, A., Klinge, A., Nedergaard, J., Siemen, D. 1998. Regulation of the activity of 27 pS nonselective cation channels in excised membrane patches from brown-fat cells. *Cell. Physiol. Biochem.* **8:**231–245

Launay, P., Feig, A., Perraud, A.-L., Scharenberg, A.M., Penner, R., Kinet, J.-P. 2002. TRPM4 is a Ca^{2+}-activated nonselective cation channel mediating cell membrane depolarization. *Cell* **109:**397–407

Montell, C., Birnbaumer, L., Flockerzi, V. 2002. The trp channels, a remarkably functional family. *Cell* **108:**595–598

Neher, E. 1992. Correction for liquid junction potentials in patch clamp experiments. *Meth. Enzymol.* **207:**123–131

Partridge, L.D., Swandulla, D. 1988. Calcium-activated non-specific cation channels. *TINS* **11**:69–72

Petersen, O.H. 2002. Cation channels: homing in on the elusive CAN channels. *Curr. Biol.* **12**:R520–R522

Schoenmakers, T.J.M., Visser, G.J., Filk, G., Theuvenet, A.P.R. 1992. Chelator: an improved method for computing metal ion concentrations in physiological solutions. *Biotechniq.* **12**:994–1000

Siemen, D. 1993. Nonselective cation channels. *EXS* **66**:3–25

Suh, H.S., Watanabe, H., Droogmans, G., Nilius, B. 2002. ATP and nitric oxide modulate a Ca^{2+}-activated non-selective cation current in macrovascular endothelial cells. *Eur. J. Physiol.* **444**:438–445

Thorn, P., Petersen, O.H. 1993. Nonselective cation channels in exocrine gland cells. *EXS* **66**:185–200

Vennekens, R., Voets, T., Bindels, R.J.M., Droogmans, G., Nilius, B. 2002. Current understanding of mammalian TRP homologues. *Cell Calcium* **31**:253–264

Zhainazarov, A.B., Doolin, R.E., Ache, B.W. 1998. Sodium-gated cation channel implicated in the activation of lobster olfactory receptor neurons. *J. Neurophysiol.* **79**:1349–1359